



Published in final edited form as:

Chem Commun (Camb). 2011 February 21; 47(7): 2149–2151. doi:10.1039/c0cc03746j.

Fe₃O₄@organic@Au: Core-Shell Nanocomposites with High Saturation Magnetisation as Magnetoplasmonic MRI Contrast Agents[†]

Eric D. Smolensky, Michelle C. Neary, Yue Zhou, Thelma S. Berquo, and Valérie C. Pierre^{*}

Department of Chemistry, University of Minnesota, 207 Pleasant Street SE, Minneapolis, MN 55455, USA

Abstract

The synthesis and characterization of core-shell Fe₃O₄@organic@Au nanoparticles displaying plasmonic behavior, high magnetism, and high relaxivity is presented. The incorporation of a thin organic layer between the two metals is crucial to maintaining the saturation magnetisation of the superparamagnetic core.

Magnetic Iron Oxide Nanoparticles (MIONs) are increasingly used as MRI contrast agents due to their high saturation magnetisation (M_S) which leads to high transverse relaxivity.¹ Likewise, gold nanoparticles have become the material of choice in imaging techniques that exploit their plasmonic properties such as dark field spectroscopy and Surface Enhanced Raman Spectroscopy (SERS).² The combination of these two materials in a single nanocomposite displaying both magnetic and plasmonic properties, a so-called magnetoplasmonic assembly,³ is particularly attractive given the complementarity in terms of resolution and 3D imaging capabilities of the plasmonic and MR imaging techniques.^{1,2} Herein we present the synthesis and characterization of magnetite@organic layer@gold core-shell nanocomposites which display high saturation magnetisation due to the presence of a thin organic layer.

Multimodal nanocomposites comprised of both iron oxide and gold components can be synthesized in either of two ways. In the first case, both nanoparticles of gold and iron oxide are embedded in a polymer or silica coating.^{3,4} This approach unfortunately results in assemblies of size typically around 150–200 nm, which are too large for cellular imaging and for most in vivo applications.⁵ Alternatively, a core-shell structure, typically with an iron oxide core and an outermost gold layer, enables the synthesis of smaller nanoparticles, typically 80 nm in diameter. Advantageously, these assemblies can also be readily functionalized with biomolecules since the chemistry of conjugation of proteins and nucleic acids to gold surfaces is well established.^{6–9} The disadvantages of these structures is twofold. First, the coating on the iron oxide core, which includes the gold layer, is typically ca. 35 nm thick or more. Since this thick coating increases the distance separating the magnetic core from the solvent water molecules, both the longitudinal and the transverse relaxivities of the material are significantly reduced.¹ Secondly, and importantly, direct coating of gold onto iron oxide nanoparticles severely decreases the saturation

[†]Electronic Supplementary Information (ESI) available: Detailed experimental procedure and characterization of the nanoparticles. See DOI: 10.1039/b000000x/

© The Royal Society of Chemistry

^aFax: (+1) 612 626 7541; Tel: (+1) 612 625 0921; pierre@umn.edu.

magnetization (on a per iron basis) of the magnetic core by 78% or more.^{9,10} This further reduces the relaxivities, and hence the potency of the nanocomposites as MR contrast agents.

The mechanism by which the gold coating decreases the saturation magnetisation of the magnetite core is presently not well understood. Similar effects have been observed in gold coated cobalt nanoparticles.¹¹ For such nanocomposites, the decrease in magnetism has been attributed to migration of gold atoms into the cobalt core. The ensuing distortion of the structure responsible for the superparamagnetic behavior resulted in a decrease in magnetisation of the cobalt core. It is possible that a similar migration of gold atoms into a maghemite or magnetite core could cause the observed decrease in M_S . If this is the case, then incorporation of an organic layer between the iron oxide core and the gold layer is expected to prevent or reduce this migration and in turn significantly increase the saturation magnetisation and relaxivity of the material.

A number of parameters should be considered in choosing this organic layer. (1) Our group,¹² among others,¹³ has demonstrated that certain organic and polymer coatings, silicates in particular,¹⁴ significantly decrease the saturation magnetisation and relaxivity of iron oxide nanoparticles. The organic coating should thus be composed of anchoring groups that do not affect the magnetism of the iron oxide core. (2) The longitudinal (r_1) and transverse (r_2) relaxivities of MIONs – a measure of the efficacy of the nanoparticles to behave as MR contrast agents – decreases as the thickness of the coating, including the organic and the gold layers, increases.¹ The organic or insulating layer should thus be kept as thin as possible.

Taking both points into consideration, the ideal composition of the organic insulator would be a monolayer of a small organic chelator which contains a phosphonate or catecholate anchoring group which can stably coordinate the magnetite core without adversely affecting its magnetism, and an amine or a thiol to enable the deposition of the outermost gold layer. 3-Aminopropylphosphonic acid fulfilled each of these requirements and was therefore used in the synthesis of the nanocomposites (Fig 1). Advantageously, according to the principle of hard and soft acids and bases, the harder phosphonic acid group of the organic layer is expected to selectively chelate the core composed of the harder iron metal, while the softer amine ligand should preferentially coordinate the softer gold. Our targeted material also contains a magnetite core 5 nm in size – a size which maximizes the r_1/r_2 ratio for increased MR contrast¹ – and a 7.5 nm thick gold layer, thick enough to observe the characteristic surface plasmon bands in the visible spectra.²

The assembly was synthesized as follows (Fig 1). Oleic-acid functionalized magnetite nanoparticles of size 4.8 ± 1.1 nm were synthesized from thermal decomposition of $\text{Fe}(\text{acac})_3$ in the presence of oleic acid and oleylamine according to the procedure developed by Wang and coworkers (Fig 2a).¹⁵ The XRD (Fig 3) and UV-visible (Fig 4) spectra are characteristic of magnetite nanoparticles; the line broadening observed in the XRD spectra is indicative of the small size of the nanoparticles. Importantly, this procedure enables the synthesis of iron oxide particles with high saturation magnetisation of $92 \text{ Am}^2/\text{kg}$ (Fig 5). The hydrophobic oleic acid coating was then replaced with the hydrophilic 3-aminopropylphosphonic acid according to a biphasic procedure as previously reported.¹² Successful refunctionalization was confirmed by IR spectroscopy (see Supplemental Information). 3-Aminopropylphosphonic acid does not noticeably affect the size (4.9 ± 1.0 nm), the shape (Fig 2b), or the UV-visible spectrum (Fig 4). The magnetization is also little affected by the new organic layer. The nanoparticles remain superparamagnetic and their M_S , on a per mass of magnetite basis, decreases to $57 \text{ Am}^2/\text{kg}$ (Fig 5).

Deposition of the gold layer onto the amine-coated MIONs was achieved by sonicating the nanoparticles in an aqueous solution of HAuCl_4 in the presence of 7 equivalents of the reducing agent sodium citrate. A similar procedure was followed by Wei to layer gold onto silica-coated nanoparticles.⁸ The resulting nanoparticles are significantly larger, with a size of 20.6 ± 7.8 nm, and more spherical compared to the mostly cubic oleic acid-coated iron oxide starting material (Fig 2c). The increase in size of the nanoparticles corresponds to the addition of a gold layer 7.5 nm thick. It should be noted that this procedure does not enable uniform coating of gold layers of the same thickness onto each nanoparticle. As a result, there is a significant polydispersity observed in the final product.

The UV-visible spectra of the nanocomposite shows a distinct band centered at 528 nm characteristic of the surface plasmon band of gold nanoparticles, which is present neither in the spectra of the Fe_3O_4 @oleic acid precursor nor in that of the Fe_3O_4 @organic intermediate. This band is broad, a further indication of the polydispersity in thickness of gold coatings.² Gold coating on the iron oxide nanoparticles, as opposed to the formation of solid gold nanoparticles separate from the MIONs, is further supported by the XRD. In the powder X-Ray diffraction, the bands characteristic of magnetite no longer appear in the final material. Instead the three bands attributed to solid gold are present at $2\theta = 44.6, 52.0$ and 76.7 (JCPDS #89-3697, Fig 3). The absence of bands corresponding to magnetite in the XRD of the final product provides further indication that all iron oxide nanoparticles are coated with gold and that the gold layer is at least 2 nm thick.¹⁶

Significantly, the presence of the thin organic coating between the magnetite core and the outermost gold layer efficiently protects the magnetism of the core. As can be seen in the magnetic hysteresis plot (Fig 5), not only does the iron oxide core of the assembly maintain its superparamagnetic character, but the saturation magnetisation of the Fe_3O_4 @organic@gold nanoparticles remains very high at $81 \text{ Am}^2/\text{kg}$. The presence of 3-aminopropylphosphonate limits the decrease in M_S to merely 12%; the M_S of the nanocomposite is four times higher than if the organic layer was not present.⁹ The incorporation of the thin organic coating thus enables the synthesis of heterometallic assemblies with high magnetism.

Together with the high saturation magnetisation of the iron oxide core, the thinness of the organic plus gold layers makes the nanocomposite a very potent MR contrast agent. The transverse relaxivity, r_2 , of the Fe_3O_4 @organic@Au nanoparticles in water is $90.9 \text{ mM}_{\text{Fe}}^{-1}\text{s}^{-1}$ at neutral pH, 37°C and 60 MHz. The longitudinal relaxivity is $r_1 = 10.3 \text{ mM}_{\text{Fe}}^{-1}\text{s}^{-1}$. This is higher than the value of most USPIOs (Ultra Small Particles of Iron Oxides).¹⁷ In comparison, the clinical USPIO Sinerem[®] (Guerbet, France) which is also comprised of magnetite cores 4-5 nm in diameter but which is instead coated with a 20 nm thick dextran layer, displays a significantly lower r_2 of $53.1 \text{ mM}_{\text{Fe}}^{-1}\text{s}^{-1}$.¹⁸

In conclusion, we have demonstrated that the incorporation of a thin organic coating containing efficient iron oxide and gold chelators can significantly increase the saturation magnetisation of core-shell iron oxide@gold nanoparticles. The resulting high relaxivity of the nanocomposites, together with the small, compact structure of the assemblies and their characteristic plasmonic behavior, renders Fe_3O_4 @organic@gold an attractive alternative to current magnetoplasmonic agents for multimodal cell imaging.

Supplementary Material

Refer to Web version on PubMed Central for supplementary material.

Acknowledgments

This work was supported by the NIH-CBITG and the University of Minnesota, Twin-Cities. Support to MCN from NSF-REU 0851234 and to YZ from UMN UROP is gratefully acknowledged. Parts of this work was carried out in the Institute of Technology Characterization Facility, UMN, a member of the NSF-funded Materials Research Facilities Network (www.mrfn.org), and at the Institute for Rock Magnetism, UMN. The IRM and its instrumentations are funded by the Earth Science Division of the NSF, the W. M Keck foundation and UMN. We thank Lee Penn for the use of the X-ray diffractometer.

References

1. Laurent S, Forge D, Port M, Roch A, Robic C, Vander Elst L, Muller RN. *Chem. Rev.* 2008; 108:2064–2110. [PubMed: 18543879]
2. Daniel MC, Astruc D. *Chem. Rev.* 2004; 104:293–346. [PubMed: 14719978]
3. Chen W, Xu N, Xu L, Wang L, Li Z, Ma W, Zhu Y, Xu C, Kotov NA. *Macromol. Rapid Commun.* 2010; 31:228–236.
4. Stoeva SI, Huo F, Lee J-S, Mirkin CA. *J. Am. Chem. Soc.* 2005; 127:15362–15363. [PubMed: 16262387] Chenjie X, Jin X, Don H, Chao W, Nathan K, Edward GW, Jeffrey RM, Chin YE, Shouheng S. *Angew. Chem., Int. Ed. Engl.* 2008; 47:173–176. [PubMed: 17992677]
5. Thorek DLJ, Tsourkas A. *Biomaterials.* 2008; 29:3583–3590. [PubMed: 18533252]
6. Melancon MP, Lu W, Li C. *Mrs Bulletin.* 2009; 34:415–421.
7. Zhao X, Cai Y, Wang T, Shi Y, Jiang G. *Anal. Chem.* 2008; 80:9091–9096. [PubMed: 19551935] Qiaozhen Y, Minmin S, Yunan C, Mang W, Hong-zheng C. *Nanotechnology.* 2008:265702. Im I, Peter N, Hye-Young P, Xin W, Lingyan W, Derrick M, Chuan-Jian Z. *Nanotechnology.* 2008:305102. Lu Q, Yao K, Xi D, Liu Z, Luo X, Ning Q. *J. Magn. Mater.* 2006; 301:44–49.
8. Wei W, Quanguo H, Hong C, Jianxin T, Libo N. *Nanotechnology.* 2007:145609.
9. Wang L, Park H-Y, Lim SII, Schadt MJ, Mott D, Luo J, Wang X, Zhong C-J. *J. Mater. Chem.* 2008; 18:2629–2635.
10. Chiang IC, Chen DH. *Adv. Funct. Mater.* 2007; 17:1311–1316.
11. Cheng G, Hight Walker AR. *J. Magn. Mater.* 2007; 311:31–35.
12. Smolensky ED, Park H-YE, Berquo TS, Pierre VC. *Contrast Media Mol. Imaging.* in press.
13. Daou TJ, Greneche JM, Pourroy G, Buathong S, Derory A, Ulhaq-Bouillet C, Donnio B, Guillon D, Begin-Colin S. *Chem. Mater.* 2008; 20:5869–5875. Sahoo Y, Pizem H, Fried T, Golodnitsky D, Burstein L, Sukenik CN, Markovich G. *Langmuir.* 2001; 17:7907–7911. Yee C, Kataby G, Ulman A, Prozorov T, White H, King A, Rafailovich M, Sokolov J, Gedanken A. *Langmuir.* 1999; 15:7111–7115.
14. Herea DD, Chiriac H. *Optoelectron. Adv. Mat.* 2008; 2:549–552.
15. Sun S, Zeng H, Robinson DB, Raoux S, Rice PM, Wang SX, Li G. *J. Am. Chem. Soc.* 2003; 126:273–279. [PubMed: 14709092]
16. Xu Z, Hou Y, Sun S. *J. Am. Chem. Soc.* 2007; 129:8698–8699. [PubMed: 17590000]
17. Aggregates of iron oxide nanoparticles, known as SPIOs, have significant higher transverse relaxivities. See ref 1 for details.
18. Rohrer M, Bauer H, Mintorovitch J, Requardt M, Weinmann HJ. *Invest. Radiol.* 2005; 40:715–724. [PubMed: 16230904]

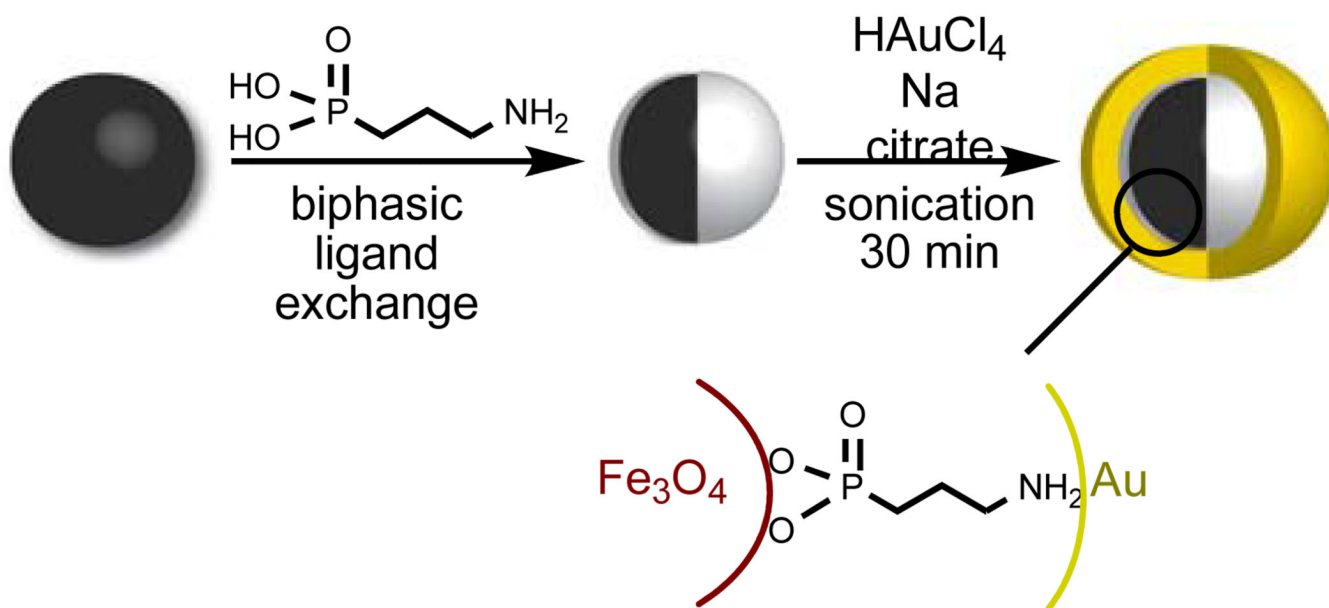


Figure 1. Synthesis and idealized structure of Fe₃O₄@organic@Au nanocomposites.

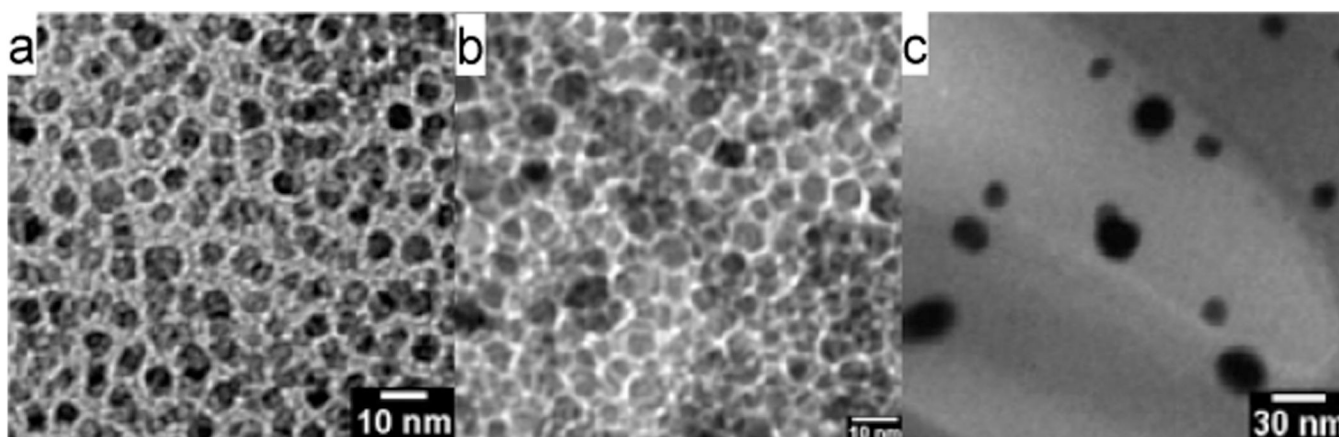


Figure 2. Transmission Electron Micrographs of a) Fe_3O_4 @oleic acid precursor, b) Fe_3O_4 @organic, c) Fe_3O_4 @organic@Au.

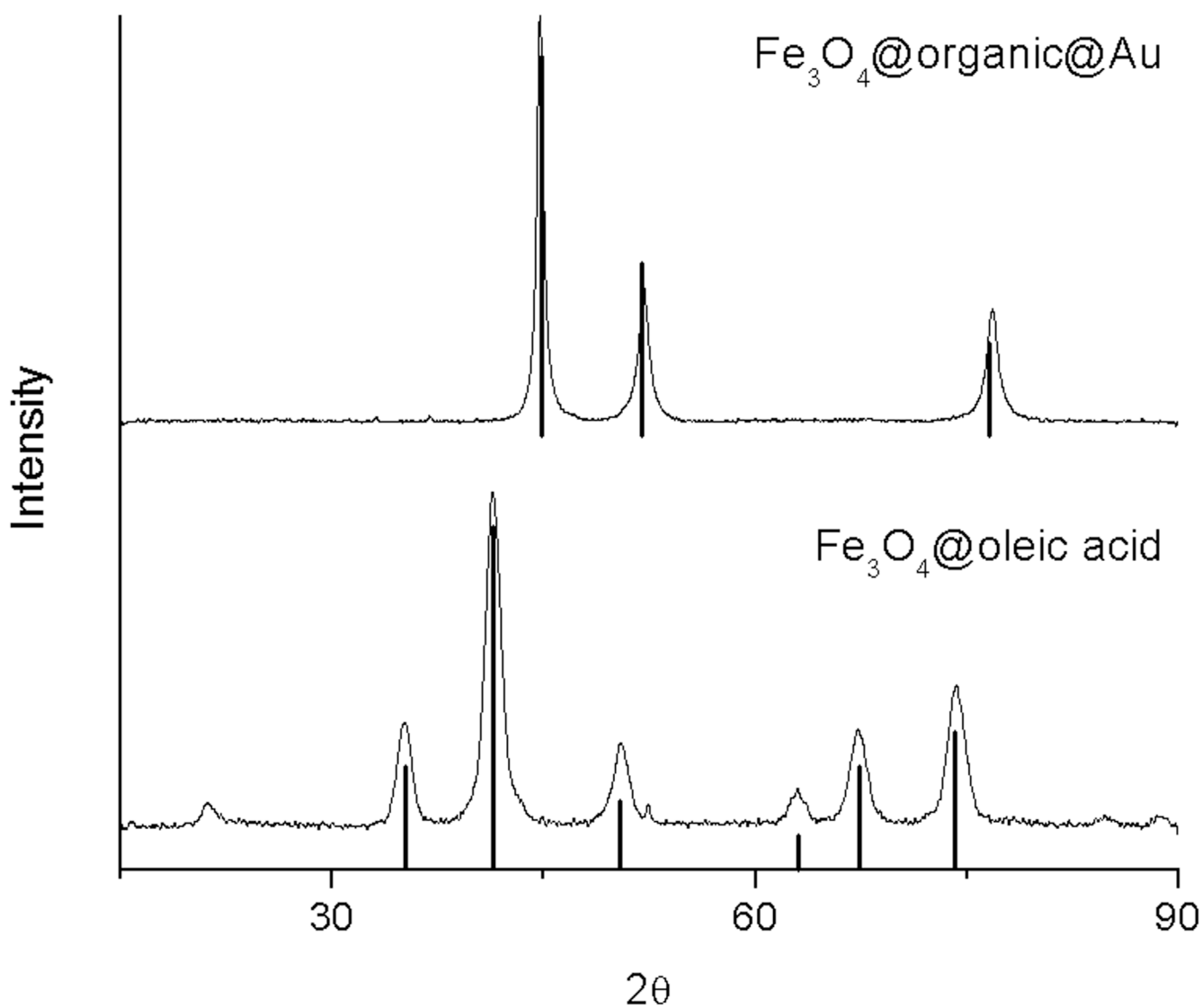


Figure 3. X-ray diffraction patterns of the Fe₃O₄@oleic acid precursor (bottom) and Fe₃O₄@organic@Au (top). The theoretical diffraction patterns of magnetite (bottom, JCPDS #19-629) and gold (top, JCPDS #89-3697) are indicated as bars.

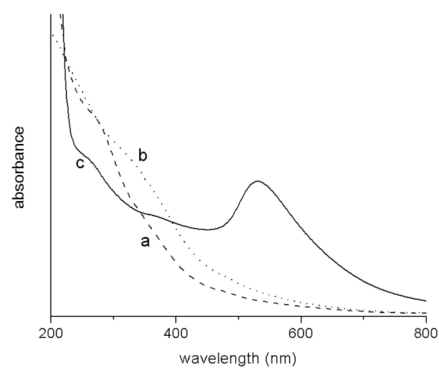


Figure 4. UV-visible spectra of a) Fe₃O₄@oleic acid precursor (dashed line), b) Fe₃O₄@organic intermediate (dotted line) and c) Fe₃O₄@organic@Au (solid line).

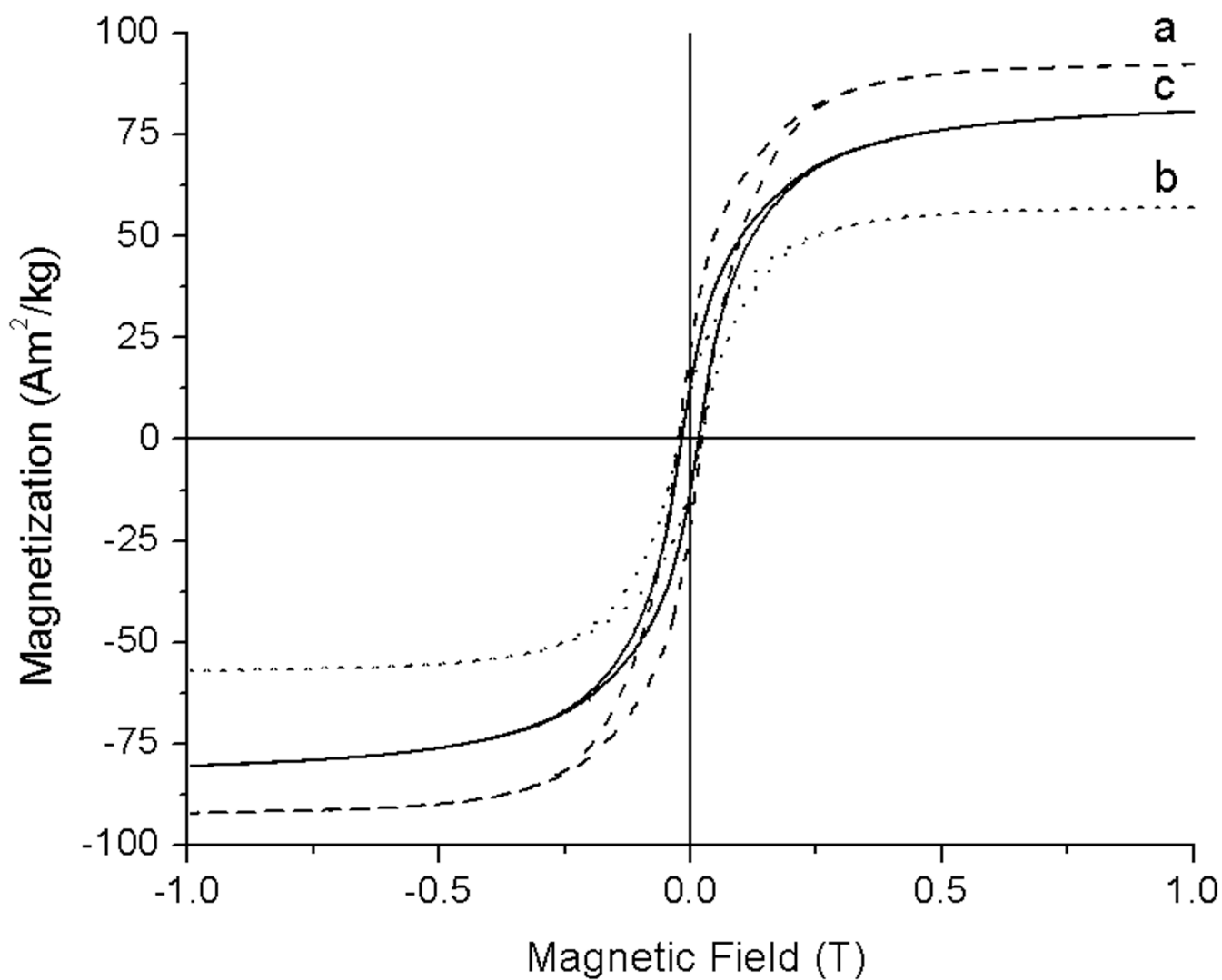


Figure 5. Hysteresis loops of a) Fe_3O_4 @oleic acid precursor (dashed line), b) Fe_3O_4 @organic intermediate (dotted line) and c) Fe_3O_4 @organic@Au at 4K (solid line).